

Dynamic real-time volumetric correction for tipping-bucket rain gauges

Przemysław Sypka

AGH University of Science and Technology, Department of Electronics, Al. Mickiewicza 30, 30-059, Kraków, Poland



ARTICLE INFO

Keywords:

Tipping-bucket rain gauge
Dynamic volumetric correction
Systematic error suppression
Real time correction
Precipitation measurement
Hydrological monitoring

ABSTRACT

Tipping bucket rain gauges are the most popular devices for determining rainfall intensity and precipitation depth. Even though application of a tipping bucket gauge presupposes calibration, they are susceptible to various random, mechanical, and systematic errors. In general, precipitation measurements may be underestimated by 5% to 40%. This paper presents a method of determining volumetric correction that compensates for systematic errors caused by variable rainfall intensity. The main goal of this study was to develop a suitable mathematical model that can be readily implemented in real time during field measurements, including the possibility of compensation of each individual tip. The developed algorithm is based on a “tip interval” recording method; this is in contrast to the standard measurement method, which is based on “tip count” and nominal tip volume. Such a solution may be applied to any kind of tipping-bucket rain gauge and can be effortlessly implemented in modern digital data loggers. In addition, smaller canisters may be used in a seesaw-like mechanism that provides accurate measurements over a considerably wider range of rainfall rates, even including extreme rainfall. During meticulous laboratory experiments, various tipping buckets with nominal volumes of 3 cm³, 4 cm³, 5 cm³, 10 cm³ and 200 cm³ were tested over a wide range of simulated precipitation rates from 8 mm·h⁻¹ to 500 mm·h⁻¹. The extent of error reduction was 5.2%, 11.4%, 17.7%, 25.8% and 37.7% for rainfall intensities of 50 mm·h⁻¹, 100 mm·h⁻¹, 200 mm·h⁻¹, 300 mm·h⁻¹ and 500 mm·h⁻¹, respectively (assuming that the nominal volume of the tipping bucket was 4 cm³ and the collection area of the rain gauge was 200 cm²). Besides scrupulous laboratory tests, the presented algorithm was verified during field measurements at 29 research sites located in a temperate climate region in two vegetation zones: foothills and lower montane. The results of this research will considerably enhance the accuracy of the precipitation data that are essential in various hydrological studies.

1. Introduction

Appropriate measurements of precipitation, its intensity, depth, and spatial distribution are a fundamental issue in meteorology, climate monitoring, and various hydrological and ecological applications (Eagleson, 1970; Geiger et al., 1995). In typical approaches, rainfall-measuring devices are placed at a specific height, normally 0.5 m–1.5 m above the ground. There are three major standard classes of precipitation sensors: manual rain gauges, tipping-bucket rain gauges, and weighing rain gauges (WMO, 2008). However, novel approaches are based on optical infrared sensors. Tipping-bucket rain gauges are the most popular because they are simple, robust, easily adaptable to different data loggers, and make accurate point measurements available. Furthermore, tipping-bucket rain gauges are usually based on an uncomplicated magnetic reed switch, thus they have zero power consumption and can be effortlessly installed in remote areas.

Due to measurement conditions (i.e. size and shape of sensors and height of measurement) various random, mechanical, and systematic errors may be observed (Sevruk and Chvíla, 2005; Ren and Li, 2007;

Sevruk et al., 2009; Colli et al., 2013, 2014). Random errors are a result of unpredictable factors such as human error, damage to sensors, or interference from fauna and flora (for example, debris blocking the gauge orifice). Random errors can be also caused by a small collection area (200 cm² to 500 cm²). Systematic and mechanical errors may be attributable to incorrectness of catching and counting. Mechanical errors involve rolling resistance of the shaft, imbalance of tipping buckets, and limited tipping rate. The dominant systematic error is caused by wind turbulence above the gauge funnel (Nešpor and Sevruk, 1999), which increases with the height of the instrument's installation (Sevruk, 1981). Other inaccuracies arise from wetting loss to the internal wall of the gauging funnel, evaporation, and splashing. Some systematic errors may be trimmed by correction for wind speed and temperature measured close to the rain gauge (Michelson, 2004; Stisen et al., 2012). In general, the precision of precipitation measurements may be underestimated by 5% to 40% (Legates and Willmott, 1990; Groisman and Legates, 1994; Humphrey et al., 1997; Hoffmann et al., 2016).

Application of a tipping-bucket gauge presupposes a calibration, the process of which involves two procedures: static calibration and

E-mail address: sypka@agh.edu.pl.

<https://doi.org/10.1016/j.agrformet.2019.02.044>

Received 12 July 2018; Received in revised form 26 February 2019; Accepted 28 February 2019

0168-1923/ © 2019 Elsevier B.V. All rights reserved.

dynamic calibration. Volumetric (static) adjustment means fine-tuning the water volume required to tip the bucket. The adjusted volume of the tip defines the resolution of a given tipping-bucket gauge. During dynamic calibration the tipping bucket is in motion and the volumetric correction for rainfall rates is usually examined. Information about volumetric errors may often be found in the specification data sheet of a tipping-bucket rain gauge; for example, 2% for rainfall intensity up to $25 \text{ mm}\cdot\text{h}^{-1}$, 3% for rainfall intensity up to $50 \text{ mm}\cdot\text{h}^{-1}$ (DAVIS, 7852M; YOUNG, 52202). A number of static and dynamic calibration methodologies may be found in the recent literature, the majority of which focus on mechanical aspects (Sevruk, 1996; Fankhauser, 1998; Bergmann et al., 2001; Vasvári, 2005; Borup et al., 2016; Hoffman et al., 2016); other methods are based on statistical techniques (Molini et al., 2005; Seo et al., 2014). Additionally, there have been some studies to improve the shape of this instrument (Seibert and Morén, 1999; DAVIS, 6463). Despite the effort put into the calibration process, only a few works have tested the relationship between volumetric and dynamic adjustments (Shedekar et al., 2016). Nevertheless, all these methods rely on data and statistics produced as part of each specific calibration process and therefore cannot be implemented in real time during field measurements.

This paper presents a methodology to improve the accuracy of tipping-bucket rain gauges by suppression of the systematic volumetric error caused by precipitation intensity, i.e. variable tip intervals. The main goal of this study was to develop a suitable mathematical model that could be readily implemented in real time during field measurements. The second aim was that the elaborated technique should ensure the possibility of fine tuning for every particular tip of a bucket. The presented procedure was tested during extended field point measurements in a temperate climate region, mainly in two vegetation zones: foothills and lower montane. The research sites were located under the canopies of tree stands of various species (spruce, fir, pine, and beech) under different silvicultural practices, such as the selection forest system and the stepwise cutting and clear-cutting systems. Installation of the rain gauge under the canopy minimized errors caused by wind turbulence above the funnel gauge; however, the recorded rainfall rates might have been lower compared to open field sites.

2. Materials and methods

In standard approaches, a small pipette is used during static calibration to determine the nominal volume of tipped water. Calibration screws are used to equalize the volumes of the left and right canisters and to obtain the predetermined resolution of rainfall depth by the following formula: $(1)D_{RNFL} = 10 \cdot \frac{V_0}{A} = 10 \cdot \frac{4}{\pi \cdot D^2} \cdot V_0$ where: D_{RNFL} denotes rainfall depth [mm]; V_0 is the nominal volume of the tipping bucket [cm^3]; A is the collection area of the rain gauge [cm^2]; D represents the input diameter of the catchment funnel [cm]. For dynamic calibration a meticulously calibrated peristaltic pump is usually used to obtain a set of various flow rates that models a range of rain intensities. In the presented work, due to the proposed algorithm described in Section 3, a different solution was used (Fig. 1). A level platform with a raised water container was designed. A tipping bucket mechanism ($V_0 = 4 \text{ cm}^3$) was mounted on four long adjustable screws. Such a solution was made possible by independent levelling of the seesaw-like mechanism of the tipping bucket mechanism as well as regulation of the installation height of the examined instrument over the platform. Water was supplied by a dispensing needle mounted on an adjustable extension arm to ensure the same distance from the outlet of the funnel to the tipping buckets as is in the examined gauge. Flow rate was regulated by a precision clamping screw. An auxiliary water canister with a small pump (Comet ELEGANT) maintained a constant head of water in the upper container; therefore, a steady flow rate was ensured as a result of the fixed water pressure in the dispensing needle. Every tipped volume of water was measured by a precision laboratory balance (RADWAG PS



Fig. 1. The laboratory stand used in the calibration process. Flow rate was regulated by a precision clamping screw. The constant difference between the water head in the main container and the dispensing needle ensured a steady flow rate. Every tipped volume of water was measured by a precision laboratory balance. A data logger recorded both the interval between tips and the tipped water weight (volume). A – level platform with precision laboratory balance; B – main water container with constant head of water; C – tipping bucket mechanism; D – dispensing-needle to supply water; E – precision clamping screw to regulate flow rate; F – auxiliary water canister with small pump; G – data logger.

1000/C2, $e = 1 \text{ mg}$) with the common assumption that 1 g is equivalent to 1 cm^3 of water. The precision balance was programmed to take continuous measurements with automatic data transmission through its embedded serial port (10 readings per second). A custom-made data logger recorded both the interval between tips and the tipped water weight (total mass, mean value of the last 4 measurements before the next tip). Furthermore, the aforementioned assessment allows statistical analysis of inaccuracies of subsequent tips.

2.1. Calibration measurements

First, the examined tipping bucket mechanism was statically balanced; its shaft was mounted on slide bearings that rolled without any frictional drag. The calibration screws were adjusted to ensure the same amount (weight/volume) of tipped water from both left and right canisters. Secondly, the nominal volume of the tested gauge was adjusted to 4 cm^3 , which is equivalent to a rainfall depth of 0.2 mm (assuming that the collection area equalled 200 cm^2). Various rainfall intensities were simulated by fine-tuning of the precision clamping

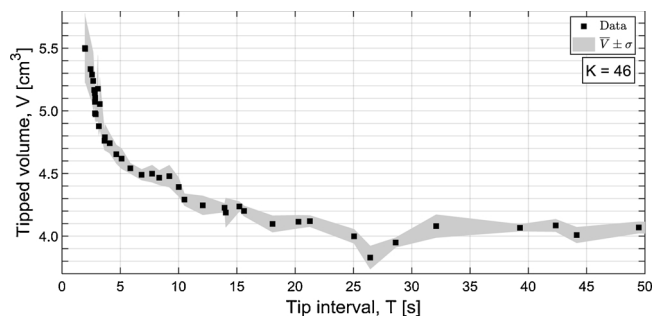


Fig. 2. The relationship between tipped water volume and tip interval over a range of simulated flow rates obtained during laboratory assessments ($V_0 = 4 \text{ cm}^3$). Each data point represents a mean value of 100 measurements taken for every simulated rainfall intensity. The grey area shows mean values with plus/minus standard deviation. K – number of cases, i.e. number of series performed during laboratory tests (For interpretation of the references to colour in this figure legend, the reader is referred to the web version of this article).

screw. The range of tipping intervals was from approximately 2 s to 89.5 s, which was roughly equivalent to a precipitation rate of $500 \text{ mm}\cdot\text{h}^{-1}$ to $8 \text{ mm}\cdot\text{h}^{-1}$ ($A = 200 \text{ cm}^2$), respectively. For every simulated rainfall intensity (46 cases in total) a series of 100 measurements was conducted. Tip interval was measured with a resolution of 1 ms; tip volume was measured to a resolution of 1 mg with a precision laboratory balance. The results, i.e. mean values from each series, are presented in Fig. 2 (the data points for $T = 78.1, 78.5, 89.5 \text{ s}$ and $V = 3.98, 4.05, 4.02 \text{ cm}^3$, respectively, are not shown). It may be observed that the tipped volume was nearly constant until tip intervals were greater than roughly 25 s (equivalent to $28.8 \text{ mm}\cdot\text{h}^{-1}$). For shorter tip intervals, the tipping bucket mechanism does not maintain an invariable volume. The amount of spilled water rises nonlinearly and is inversely proportional to the tip interval. For very small tip intervals lower than 4 s (approx. $215 \text{ mm}\cdot\text{h}^{-1}$), the dependence grows rapidly. In such instances, a tipping-bucket rain gauge may underestimate precipitation rate by more than 30%. Therefore, a standard measurement methodology based only on tip counting and nominal volume cannot be used for precision precipitation measurements.

2.2. Algorithm for dynamic volumetric correction

The non-linear relationship between tip interval and tipped volume of water presented in Fig. 2 can be modelled in the logarithmic domain (Fig. 3). Three characteristic zones may be distinguished:

The non-linear relationship between tip interval and tipped volume of water presented in Fig. 2 can be modelled in the logarithmic domain (Fig. 3). Three characteristic zones may be distinguished:

A the static tip zone – the volume of tipped water does not change;

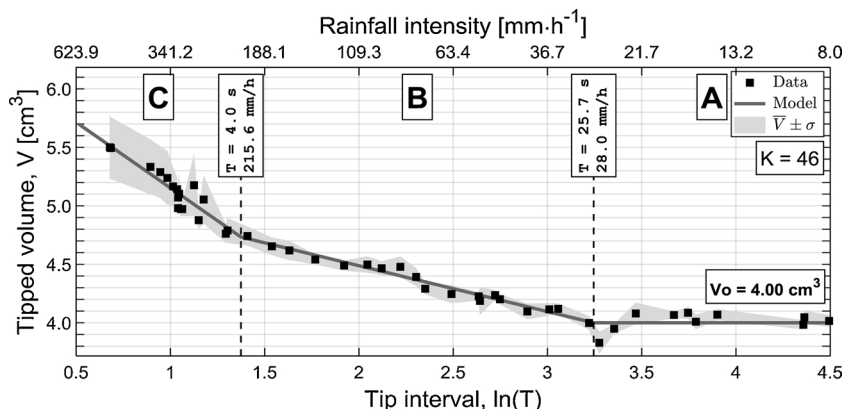


Fig. 3. The relationship between tipped water volume and tip interval over a range of simulated flow rates in the logarithmic domain. Three characteristic zones may be distinguished: A – static tip zone (volume of tipped water is constant); B – dynamic tip zone (volume collected in the bucket increases during the swing of the tipping bucket); C – rapid tip zone (tip volume is increased by the momentum of the water pouring from the funnel gauge into the bucket canister). Rainfall intensities were calculated under the assumption that the collection area equalled 200 cm^2 . Each data point (square mark) represents a mean value of 100 measurements taken for every simulated rainfall intensity. The grey area shows mean values with plus/minus standard deviation. K – number of cases, i.e. number of series performed during laboratory tests (For interpretation of the references to colour in this figure legend, the reader is referred to the web version of this article).

Table 1
Goodness-of-fit statistics for model Eq. (2).

	K	L	a	b	R	$100\cdot R^2$	σ	μ
A	10	1000	—	4.00				
B	19	1900	-0.39	5.27	0.98	96.95	0.04	0.85
C	17	1700	-1.12	6.28	0.92	85.18	0.08	1.63
Total	46	4600			0.99	98.22	0.07	1.43

K – number of cases, i.e. number of series performed during laboratory tests; L – total number of measurements in entire data set; a, b – regression coefficients; R – correlation coefficient; σ – standard deviation of estimation; μ – average error of estimation.

- standard measurement methodology based on tip counting may be used,
- B the dynamic tip zone – the volume of tipped water depends on the tip interval; this relationship may be explained by the fact that the finite swing time, i.e. the time of the swing of the tipping bucket, is constant (this depends on the mechanism and the bucket construction) and – proportionally to rain intensity – during each swing additional water might drip into the bucket until the funnel orifice is over the opposite canister,
- C the rapid tip zone – as well as the additional drops that might drip into the bucket during the tip (finite bucket swing time), the momentum of the water pouring from the funnel gauge into the bucket accelerates the moment of the tip and finally reduces the tip interval.

Based on a series of experiments, the presented relationship in the logarithmic domain can be modelled using a three-segment piecewise linear regression:

$$V = \begin{cases} 4 & \text{for } T > 25.7 \\ 5.27 - 0.39 \cdot \ln T & \text{for } 4 \leq T \leq 25.7 \\ 6.28 - 1.12 \cdot \ln T & \text{for } T < 4 \end{cases} \quad (2)$$

where V denotes the volume of tipped water [cm^3] and T is tip interval [s]. All coefficients of a three-segment piecewise linear regression and the boundary points of each zone were estimated to best fit the model function (Eq. 2) in the least-squares sense. The results of the identification of the Eq. (2) based on laboratory tests are presented in Table 1. The piecewise linear model Eq. (2) confirms that the precision of the observed relationship was over 98%. In the presented case, static calibration ($V_0 = 4 \text{ cm}^3$) can be used for tip intervals greater than 25.7 s, which is equivalent to a precipitation intensity of $28.0 \text{ mm}\cdot\text{h}^{-1}$ (assuming a collection area of 200 cm^2). Furthermore, tipping buckets with nominal volumes of $3 \text{ cm}^3, 5 \text{ cm}^3, 10 \text{ cm}^3$ and 200 cm^3 were calibrated. Despite the size of the tipping bucket, the observed relationship, i.e. the type of dynamic volumetric correction, was very similar (Fig. 4).

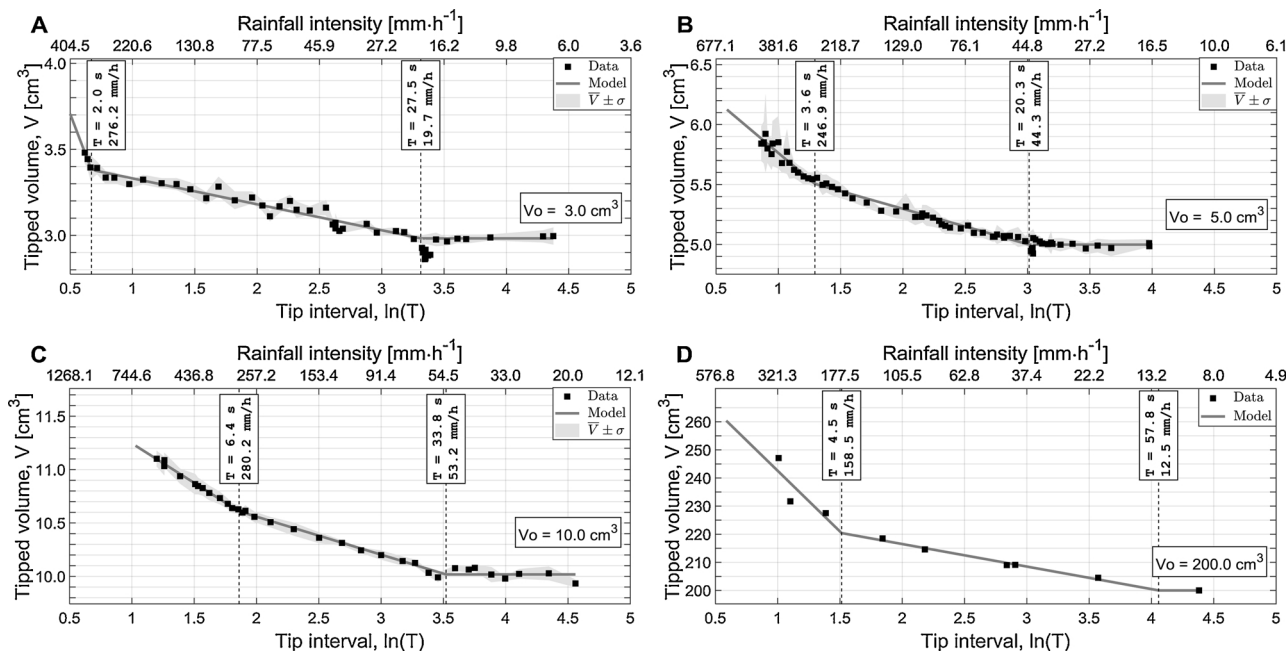


Fig. 4. The relationship between tipped water volume and tip interval over a range of simulated flow rates in the logarithmic domain for tipping buckets with nominal volumes of 3 cm³ (A), 5 cm³ (B), 10 cm³ (C) and 200 cm³ (D). Rainfall intensities were calculated under the assumption that the collection area equalled 200 cm² (A, B, C) and 1 m² (D). The grey areas show mean values with plus/minus standard deviation (For interpretation of the references to colour in this figure legend, the reader is referred to the web version of this article).

2.3. Algorithm implementation in digital data loggers

From a practical point of view, the presented model Eq. (2) cannot be readily implemented in data loggers, which are usually based on microprocessor units whose computational ability is insufficient for advanced algorithms (in this case, logarithms). Furthermore, the collected data are recorded with a predetermined resolution, so it is logical to round the measured data, both tipped volumes and tip intervals. Therefore, a lookup table including volumetric corrections (differences between actual tip volume, V , and nominal volume, V_0) may be generated based on the presented model Eq. (2). Assuming a recording resolution of $\Delta V = 0.1 \text{ cm}^3$ and $\Delta T = 0.1 \text{ s}$, the calibration curve based on Eq. (2) is presented in Fig. A1. For tip intervals greater than 22.6 s, a nominal tip volume should be used, i.e. $V = V_0$; for tip intervals shorter than 22.6 s an appropriate volumetric correction should be applied, i.e. $V = V_0 + dV$. An example lookup table with volumetric corrections is presented in Table A1. The shortest measured tip interval was 1.97 s, which is why the model function Eq. (2) produces volumetric correction values of $T < 2 \text{ s}$ which do not represent the real tip intervals of the investigated tipping bucket. Such values should be included in a lookup table to prevent unforeseen data logger errors and firmware hang-up.

2.4. Field research

The presented algorithm for volumetric correction was tested in various projects that researched water exchange balance. Two of these research projects were implemented by the Department of Forest Engineering at the University of Agriculture in Krakow, Poland, and focused on water exchange balance in forest communities, i.e. between the atmosphere, stands, and soil. During the first project, carried out from September 2011 to October 2013, 13 research sites were studied in all forest vegetation zones in the Western Carpathian Foothills at elevations from 203 m to 1197 m above mean sea level (AMSL) in various types of forest communities (beech, oak, fir, and spruce). Two rain gauges ($V_0 = 5 \text{ cm}^3$, $A = 232 \text{ cm}^2$) were installed on horizontal boom extenders mounted to a climb-up mast: the first one about 1 m above the tree tops, and the second just under the canopy. Two

additional rain gauges ($V_0 = 5 \text{ cm}^3$, $A = 232 \text{ cm}^2$) were positioned at a height of 1 m over the ground. A range of hydro-meteorological data (wind velocity, solar insolation, temperature, humidity etc.) was automatically recorded every 2 min and measurements were taken in two-week series, one series per site. The active area of the catchment funnel was 232 cm² and the nominal bucket volume was 5 cm³, i.e. one static tip was equivalent to 0.22 mm of rain. Precipitation data were measured as follows: number of tips during measurement interval, volume of tipped water (including the dynamic corrections described in Section 3), and the total volume of tipped water collected in the container under each rain gauge (measurements were taken during every maintenance visit, i.e. typically every two weeks, using a graduated cylinder with a resolution of 1 cm³). In the second project, carried out from October 2015 to July 2018, 16 research plots were located in the Beskid Sądecki Mountain Range (49°29'6.0"N, 20°46'44.3"E). The research plots were situated under the canopies of various tree stands (beech, fir and mixed) at elevations from 373 m AMSL to 870 m AMSL. During this project data were automatically recorded every 6 min throughout the whole year. At each research site a rain gauge ($V_0 = 4 \text{ cm}^3$, $A = 214 \text{ cm}^2$) was installed at a height of 1 m above ground level. These rain gauges had a collection area of 214 cm² and nominal bucket volume was 4 cm³, i.e. one static tip was equivalent to 0.19 mm of rain depth. The aforementioned mast was installed at only two sites (one full calendar year at each site, consecutively: the first site from 01-10-2015 to 25-09-2016, and the second site from 01-10-2016 to 01-10-2017). The total volume of tipped water was monitored only at rain gauges installed at ground level near a mast. The research sites in both research projects were located in a temperate climate region, mainly in two vegetation zones: foothills (up to 600 m AMSL, 13 sites) and lower montane (from 600 to 1100 m AMSL, 15 sites). From a formal perspective, one site was located in the higher montane zone (over 1100 m AMSL). The annual rainfall depth for these zones is 400 to 1200 mm a year (Stahý et al., 1986).

3. Results of field test measurements

Firstly, the overall accuracy of the rain gauge with the implemented

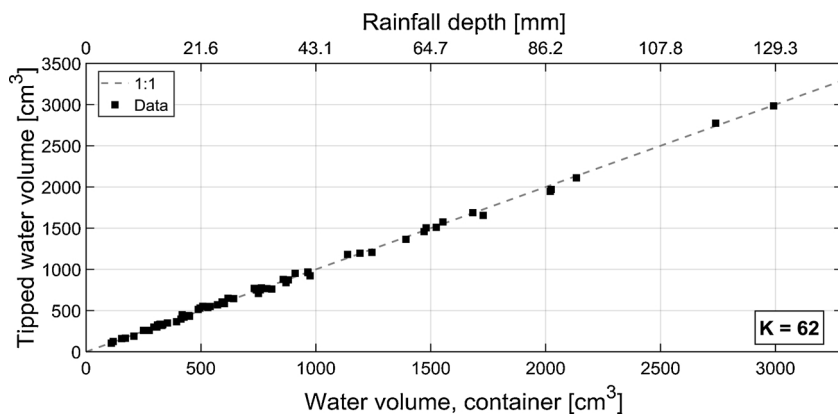


Fig. 5. Overall accuracy of measurement of tipped water volume with dynamic correction compared to volume of water collected in the canister situated under the rain gauge ($V_0 = 5 \text{ cm}^3$). Rainfall depths were calculated under the assumption that the collection area equalled 232 cm^2 . K – number of cases.

Table 2

Rain storm events recorded from the 23rd of June to 25th of August 2016 (33-day period) at a site located in Beskid Sądecki Mountains ($49^\circ 30' 51.4'' \text{N}$, $20^\circ 55' 11.3'' \text{E}$, 702 m AMSL).

Date	Start Time	End Time	Duration	V_p	V_t	D_{RNFL}	EPR_{RNFL}	AR_{RNFL}
26-07-2016	17:12	17:48	36 min	211.4	397.3	17.1	91.1	42.81
28-07-2016	11:12	12:00	48 min	143.3	253.5	10.9	61.6	13.66
29-07-2016	16:36	17:36	60 min	71.0	231.7	10.0	30.6	9.99
09-08-2016	20:00	21:24	84 min	96.6	301.8	13.0	41.6	9.29

V_p – recorded peak volume of tipped water [cm^3]; V_t – recorded total volume of tipped water [cm^3]; D_{RNFL} – rainfall depth [mm]; EPR_{RNFL} – estimated peak rainfall rate [$\text{mm}\cdot\text{h}^{-1}$]; AR_{RNFL} – average rainfall rate [$\text{mm}\cdot\text{h}^{-1}$].

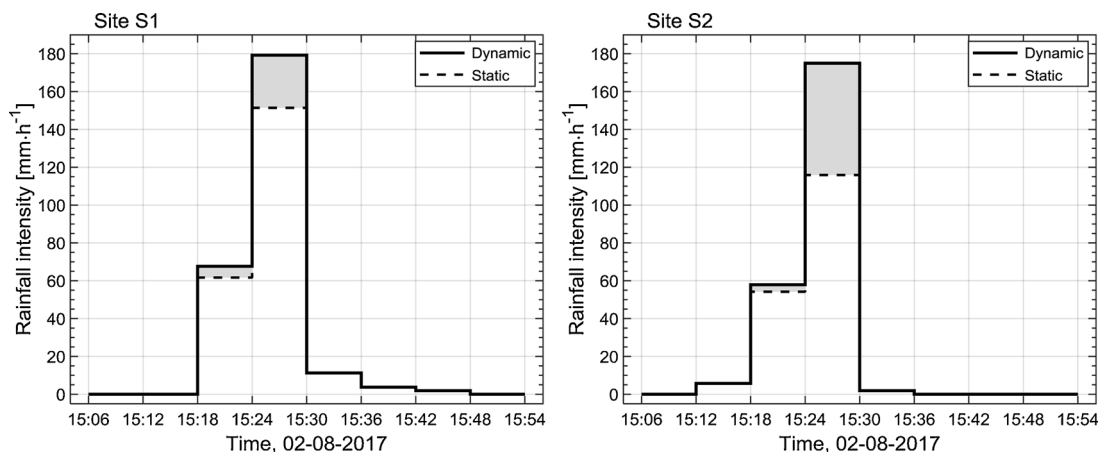


Fig. 6. An example of the same extreme rainstorm event (the highest precipitation rate recorded during test measurements) at two neighbouring sites. Grey areas show the difference between the dynamic correction and the standard static algorithm. In both cases the rain gauges ($V_0 = 4 \text{ cm}^3$, $A = 214 \text{ cm}^2$) were positioned at a height of 1 m over ground level, under a canopy: Site S1: $49^\circ 28' 24.5'' \text{N}$, $20^\circ 50' 11.3'' \text{E}$, 814 m AMSL, mixed tree stand (fir 48%, beech 49%), stepwise cutting; Site S2: $49^\circ 28' 26.3'' \text{N}$, $20^\circ 49' 27.2'' \text{E}$, 870 m AMSL, beech tree stand, Łabowiec nature reserve (For interpretation of the references to colour in this figure legend, the reader is referred to the web version of this article).

presented algorithm was examined. The volume of tipped water recorded with a data logger with embedded dynamic volumetric correction based on a lookup table ($\Delta V = 0.1 \text{ cm}^3$, $\Delta T = 0.1 \text{ s}$) was compared to the volume of water collected in the canister situated under the rain gauge. The results are presented in Fig. 5. It may be observed that measurement precision was very good even for large volumes. The highest volume of collected water was recorded from the 23rd of June to 25th of August 2016 (a 33-day period) at a site located in Beskid Sądecki Mountains ($49^\circ 30' 51.4'' \text{N}$, $20^\circ 55' 11.3'' \text{E}$, 702 m AMSL). The tipped water volume was 2984.3 cm^3 compared to 2992 cm^3 collected in the container; this is roughly 19% of annual rainfall depth at this site. The difference was 7.7 cm^3 , which means the precipitation in this period was underestimated by only 0.26%. The four rainstorm events

recorded in this period are shown in Table 2.

The highest rainfall rate was recorded on the 2nd of August 2017 at a site located in Beskid Sądecki Mountains (site S1: $49^\circ 28' 24.5'' \text{N}$, $20^\circ 50' 11.3'' \text{E}$, 814 m AMSL). This rainfall event is shown in Fig. 6 (left). This site was covered by a 23-meter-tall (on average) mixed tree stand (fir 48%, beech 49%), managed in a stepwise cutting system. The maximum amount of tipped water was 383.6 cm^3 . Taking into account the collection area of the gauging funnel (214 cm^2) and the measurement interval (6 min), it may be estimated that the peak rainfall rate was 17.93 mm per 6 min, i.e. $179.3 \text{ mm}\cdot\text{h}^{-1}$. The whole rainstorm event lasted almost 30 min, but only 2 readings (a 12-minute period) displayed its extreme nature (rainfall rate over $50 \text{ mm}\cdot\text{h}^{-1}$). Based on the standard approach, which takes only the number of tips and the

nominal volume into account, the peak rainfall rate would have been underestimated by 15.5% (grey areas in Fig. 6). The same extreme rainstorm was recorded at site S2 (49°28′26.3″N, 20°49′27.2″E, 870 m AMSL, beech tree stand, Łabowiec nature reserve), which is situated in the neighbourhood of site S1 (Fig. 6, right). The crow-fly distance between these sites was 890 m. Despite the slightly lower maximum rainfall rate at site S2 (estimated to 175.0 mm·h⁻¹), dynamic correction played a considerably greater role in this case: standard methodology would have underestimated the peak rainfall rate by 33.8%.

4. Discussion

The paper presents the analysis of the dynamic performance of a tipping-bucket rain gauge. In contrast to the previously elaborated statistical methods, which are based on already recorded data and the assumption that rainfall intensity is constant during the averaged period, i.e. the time between two consecutive measurements (Humphrey et al., 1997; Bergmann et al., 2001; Seo et al., 2014; Shedekar et al., 2016; Shimizu et al., 2018), the developed algorithm, Eq. (2), allows the application of a precision volumetric correction of tipped water for high and extreme precipitation for every particular tip in real time. The observed relationship (Fig. 3) can be expressed by the piecewise linear model Eq. (2) with very high precision (Table 1). The worst case ($100 \cdot R^2 = 85\%$) was observed for zone C (rapid tip), for which simulated precipitation intensities were greater than approx. 215 mm·h⁻¹ (extreme rain). This may be explained by the measurement conditions: water splashing from the bucket for large rainfall rates, sloshing of water in the tank on the balance pan (Fig. 1), and the stabilization time of the precision laboratory balance (around 2 s). Secondly, it may be observed (Fig. 3) that for extreme rain (rainfall intensity greater than 215.2 mm·h⁻¹) the rain gauge underestimates precipitation intensity by as much as 18% (actual tip volume equals $V = 4.73 \text{ cm}^3$ vs. nominal volume $V_0 = 4 \text{ cm}^3$). Therefore, the main disadvantage of a rain gauge based on a tipping bucket, i.e. underestimation of measured rain intensity and rainfall depth (Duchon and Biddle, 2010), can be practically eliminated (Figs. 3, 5 and 6). Consequently, tipping-bucket rain gauges with a smaller canister volume may be used to measure precipitation at higher rainfall intensities. Furthermore, the model equation based on a three-segment piecewise linear regression seems to be independent of tipping bucket size; tipping buckets with nominal volumes of 3 cm³, 4 cm³, 5 cm³, 10 cm³ and 200 cm³ were tested (Figs. 3 and 4). Therefore, it may be stated that this relationship depends on the physical properties of the mechanical construction of the small seesaw-like container and its shaft: the finite swing time of the tipping bucket mechanism and the momentum of the falling water from the gauge funnel into the bucket. It is essential to emphasize that the aforementioned benefits can be obtained only by a data recording method that takes into account the intervals between tips. The ongoing development of digital data loggers based on micro-controller units provides greater opportunities to implement such an “interval-based” algorithm equipped with an appropriate lookup table (Fig. A1, Table A1). Additionally, the presented algorithm is suitable for gauging instantaneous rainfall intensity for every single tip as a ratio of tipped volume to tip interval ($V_0 + \Delta V$)/ T . Hence, besides the mean value, maximum and minimum rainfall intensity can be recorded in each measurement.

In contrast to standard calibration routines, the developed algorithm does not require the initial setup of nominal rainfall depth by Eq. (1) because the recorded rainfall rate depends on tip volume. Only accurate determination of the nominal (static) volume of the tipping bucket is essential. However, a nominal volume that is sufficient for the predetermined resolution of rainfall depth, Eq. (1), may be practical because the vast majority of tips do not require volumetric correction (for temporary rainfall rates lower than 28 mm·h⁻¹, Fig. 3). From a formal perspective, the presented calibration method only performs dynamic calibration. However, static calibration is still possible by

preserving a sufficiently long interval between tips. Nevertheless, the crucial factors are proper balance of the tipping bucket mechanism and its precise static calibration to ensure equal volumes of the left and right seesaw-like containers. Secondly, the magnetic reed switch that is normally used to detect tips should be mounted in a shaft plane, i.e. the tipping bucket swing time (from tip triggering to reed switch contact) for both sides should be the same. Otherwise, the presented algorithm should be applied separately to the left and right buckets and the measurement method must always identify the tipping bucket. The tipping bucket swing direction may be detected by using, for example, two reed switches.

The accuracy of the presented algorithm for dynamic volumetric calibration was proved during various field measurements. Direct comparison of tipped water volume and the volume of water collected in the container confirmed the high accuracy of the results (underestimation by only 0.26% for 2992 cm³ of water collected in the container, Fig. 5). Taking in account the measurement conditions, i.e. evaporation, moistening of the hose between the rain gauge and container, and the pouring of water from the container into the graduated cylinder, such inaccuracies may be ignored. In contrast, using a standard algorithm based on only the nominal volume of the tipped water, the difference would have been 112 cm³, which is a 3.7% underestimation; this is the typical precision of standard rain gauges. Nevertheless, it should be noted that over such a long period of time (33 days) there were mainly light rains for which the presented dynamic correction was not used. Although the average rainfall intensities suggest that a dynamic volumetric correction might have been used only during the first rain storm (Table 2, average rainfall rate over 30 mm·h⁻¹), detailed analysis indicates that a dynamic volumetric correction was used during every storm event (estimated peak rainfall rates greater than 30 mm·h⁻¹ within the measurement period). During the most extreme rainfall recorded on the 2nd of August 2017, the standard approach, which takes only the number of tips and the nominal volume into account, would have underestimated the peak rainfall rate by 15.5% and 33.8% at sites S1 and S2, respectively (grey areas in Fig. 6). Furthermore, data recorded at site S2 shows that 374.5 cm³ of water was collected in 62 tips within 6 min. The detailed analysis based on only average values suggests that mean tip volume was 6.0 cm³ (compared to the nominal volume of 4 cm³), therefore the mean tip interval was 1.3 s (Table A1). Thus, it may be estimated that this peak rainstorm lasted approximately 80.6 s and the rainfall rate was 13 mm per minute (approx. 780 mm·h⁻¹). As a result of this violent rainstorm, about 40% of the tree stand was destroyed in the neighbourhood of site S2. It should be also noted that for such short tip intervals, $\ln(1.3) = 0.25$, the rain gauge was in zone C (the rapid tip zone, Fig. 3) where dynamic correction may be only estimated. It may be assumed that water poured through the unblocked funnel orifice at its maximum possible flow rate. On the contrary, at site S1, where a greater rainfall rate was logged, no tree stand damage was found. The average tip interval was around 3.9 s at this site (383.6 cm³, 81 tips), hence the maximum rainfall rate was 3.4 mm·min⁻¹ (approx. 204.3 mm·h⁻¹).

It is important to remember that tipping bucket mechanisms are not resilient to many environmental factors. During the presented field measurements, rain gauges were installed under canopies; this exposed them to clogging of the gauge orifice by debris, for example beech nut cupules in spring and honeydew and needles from fir tree stands in summer. Secondly, the tipping bucket mechanism is not hermetically sealed, therefore it is vulnerable to spider webs and insect nests – wasp nests were the most common in the presented field measurements. Even though all rain gauges were meticulously cleaned during maintenance (usually every two weeks), blockages in the gauge orifice were unavoidable. Under such adverse circumstances the presented algorithm also proved its usefulness. A self-unblocking rain gauge event is shown in Fig. 7. Firstly, as a result of leakage from a clogged catchment funnel, series of tips that lasted several days could be observed (Fig. 7A). Next, an ‘extreme rainfall’ event was recorded (Fig. 7B). Similarly, the

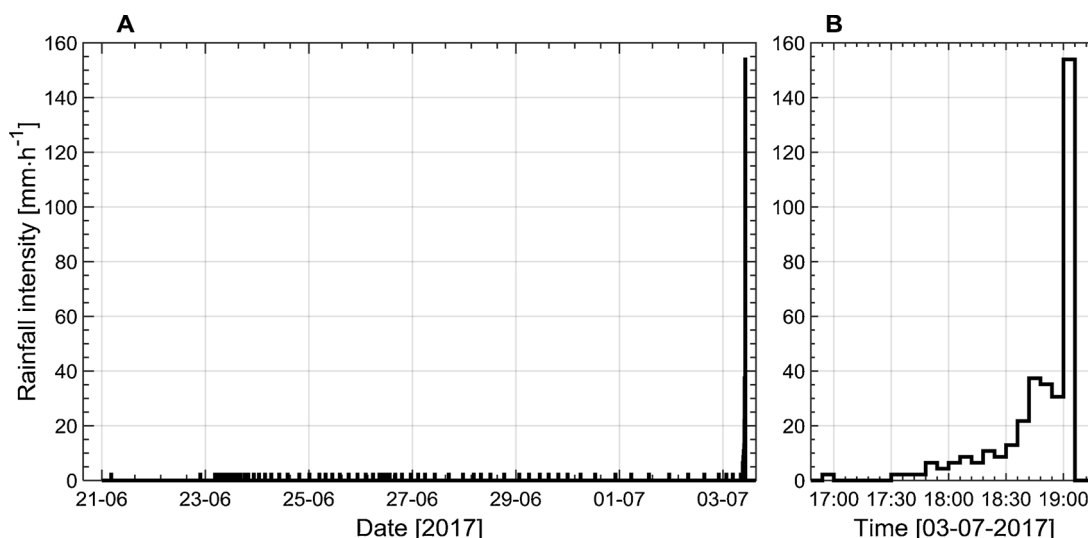


Fig. 7. A self-unblocking event of a rain gauge. Firstly, as a result of leakage from a clogged catchment funnel, a series of tips that lasted several days could be observed (A). Next, an ‘extreme rainfall’ event was recorded (B).

Table 3

The highest water volumes per 6 min, recorded during emptying of clogged rain gauges during maintenance ($V_0 = 4 \text{ cm}^3$).

Date and time	V_p	N_p	\bar{T}	dV	$\frac{dV}{V_0}$ [%]	EPR_{RNFL}
09-09-2016 15:30	1195.4	182	2.0	1.5	37.5	558.6
23-07-2016 10:12	1065.5	138	2.6	1.2	30.0	497.9

V_p – peak volume of tipped water [cm^3]; N_p – number of counts; \bar{T} – estimated mean tip interval; dV – volumetric correction (Table A1); EPR_{RNFL} – estimated peak rainfall rate [$\text{mm}\cdot\text{h}^{-1}$] (only for comparative purposes).

presented algorithm was used to measure water volume collected in clogged rain gauges during maintenance. The highest volumes recorded during emptying of clogged rain gauges during maintenance in the course of field measurements are presented in Table 3. Although such data cannot be used to estimate rainfall rates, they are critical when estimating monthly or annual precipitation at a given site (Habib et al., 2008; Hoffmann et al., 2016).

An observation worth extended research concerns the observed characteristic notch on the calibration curve. This phenomenon occurs just between the static tip zone and the dynamic tip zone in a very narrow range of flow rates (Figs. 3 and 4A, B). Furthermore, it was observed that the tipping bucket wobbled slightly in these specific intervals. Every drop of water that fell into the tipping bucket caused a tiny tilt of the seesaw-like container, after which it returned to its stable position. After a few additional drops the tipping bucket executed a complete swing, but the swing trigger moment was not easily identifiable because the ‘foot’ of the opposite seesaw-like cylinder was already very close to the calibration screw. This behaviour is presented in supplemental video (Vid.1). After a series of additional tests, it was discovered that this phenomenon depends on the drop size and the elevation of the dispensing needle over the seesaw-like canisters. As a result of such irregular activity of the tipping bucket mechanism, a notch occurred, i.e. an unexpected decrease in the tipped volume. Although it cannot be modelled based on standard regression methods (Shimizu et al., 2018), an appropriate adjustment may be added to the lookup table. The improvements required to avoid this rapid variation in volume should be possible after a series of more accurate laboratory measurements. Such exact measurements should be performed for each individual tipping-bucket rain gauge, with more points around the observed notch. In the presented survey, a simple method based on a



Fig. 8. A large drop formed at the edge of a seesaw-like container as a result of incomplete water outpour.

clamping screw and constant water pressure difference was used to obtain a given flow rate (Fig. 1). Concerning the laboratory data (Colli et al., 2013, 2014), a method combining a precalibrated high-precision peristaltic pump with a precision laboratory scale may be most appropriate. A peristaltic pump could ensure precision generation of a range of flow rates that simulate different rainfall intensities, and a laboratory scale would precisely measure the volume of tipped water. Additionally, it may be essential to uniformly sprinkle the internal walls of the catchment funnel to allow drops to form freely at the funnel orifice that are of a typical size for a given rain gauge because drop size

is another source of random errors in precipitation measurements. The swing of the tipping bucket is triggered by the appropriate weight of water collected in it. The size of the drops that fall into the tipping bucket from the gauge orifice vary, thus the water mass needed to trigger the swing is usually exceeded slightly. During laboratory measurements, dispensing needles with various diameters that formed drops of varying size were tested. In the end, a dispensing needle with an inner diameter of 1.5 mm was used. A nominal volume ($V_0 = 4 \text{ cm}^3$) was achieved during static calibration after 104 drops had been collected, therefore it may be expected that the accuracy of water mass needed to trigger a swing was 1%.

One of the most important issues that is not mentioned in the literature is the shape/profile of the tipping bucket and its coating layer. A single tip is triggered when the gravitational forces of the tipping bucket and the water collected in one cylinder lose their stable equilibrium. Therefore, even some amount of dirt or sediment accumulation on the tipping bucket can disturb it, especially if small volumetric corrections (0.1 cm^3) should be applied (Fig. 3, Fig. A1, Table A1). During laboratory measurements it was noted that there was a tendency for water to form a large drop at the end of the tipping tank (Fig. 8). Such a large water mass located far away from the shaft disturbs the tipping bucket balance and significantly changes its behaviour: the unpredictable increase of water volume in the opposite bucket is needed to trigger a swing. Such random errors, i.e. variable drop size at the edge of the tipping cylinder, cannot be compensated for with any calibration algorithm or frequent recalibration (Humphrey et al., 1997; Habib et al., 2001; Shimizu et al., 2018). Therefore, besides general recommendations about installation of tipping-bucket rain gauges and their maintenance (La Barbera et al., 2002; Shedekar et al., 2016), tipping buckets should be built with hydrophobic materials to ensure that all water efficiently flows out of the tanks. In the presented survey, the interior parts of the seesaw-like buckets were coated with a water-repellent substance (RUST-OLEUM NEVERWET MULTI-SURFACE) that completely solved the problem. However, in the course of field measurements it was found that due to dirt and sediment accumulation, such a coating layer should be refurbished at least once a year.

Appendix A. Lookup table including volumetric corrections

In practical approaches, a lookup table containing volumetric corrections (differences between actual tip volume, V , and nominal volume, V_0) is usually applied. Assuming a recording resolution of $\Delta V = 0.1 \text{ cm}^3$ and $\Delta T = 0.1 \text{ s}$, the calibration curve based on Eq. (2) is presented in Fig. A1. An example lookup table with volumetric corrections is presented in Table A1.

5. Conclusions

A thorough understanding of the dynamic performance of tipping-bucket rain gauges would considerably enhance the accuracy of precipitation data. In terms of the analysed data, the revealed dynamic volumetric correction can be used in any tipping-bucket rain gauge. The major difference is that the standard measurement algorithm, which is based on nominal tip volume, should be changed to an ‘interval-based’ method. Such a measurement technique can be applied for every particular tip in real time and underestimation of measured rain intensity and rainfall depth can be practically eliminated. Based on the presented data, the extent of error reduction was 5.2%, 11.4%, 17.7%, 25.8% and 37.7% for rainfall intensities of $50 \text{ mm}\cdot\text{h}^{-1}$, $100 \text{ mm}\cdot\text{h}^{-1}$, $200 \text{ mm}\cdot\text{h}^{-1}$, $300 \text{ mm}\cdot\text{h}^{-1}$ and $500 \text{ mm}\cdot\text{h}^{-1}$, respectively ($V_0 = 4 \text{ cm}^3$, $A = 200 \text{ cm}^2$). Secondly, an ‘interval-based’ measurement algorithm may be readily applicable to modern digital data loggers. Furthermore, an appropriate lookup table with volumetric corrections may be reprogrammed after a rain gauge is exchanged, or after more precise laboratory tests. In addition, smaller containers may be used in the seesaw-like mechanism to provide more accurate measurements over a considerably wider range of rainfall rates, even for extreme rainfall. Proper resolution and correctness of extreme rainfall rate and depth is a key factor that effects various hydrological studies, including the prediction of soil erosion and flash floods. However, correct installation on a properly levelled anti-sway platform and suitable maintenance, i.e. frequent and meticulous cleaning of the funnel orifice, inner containers, and the bucket mechanism, are still critical to assure the high accuracy and reliability of precipitation data measured by tipping-bucket rain gauges. Furthermore, it is recommended to coat the interior parts of the seesaw-like containers with a water-repellent substance to ensure complete evacuation of water from the tipping bucket.

Acknowledgements

The proposed algorithm is subject to patent protection in the Polish Patent Office: No. P-425 442.

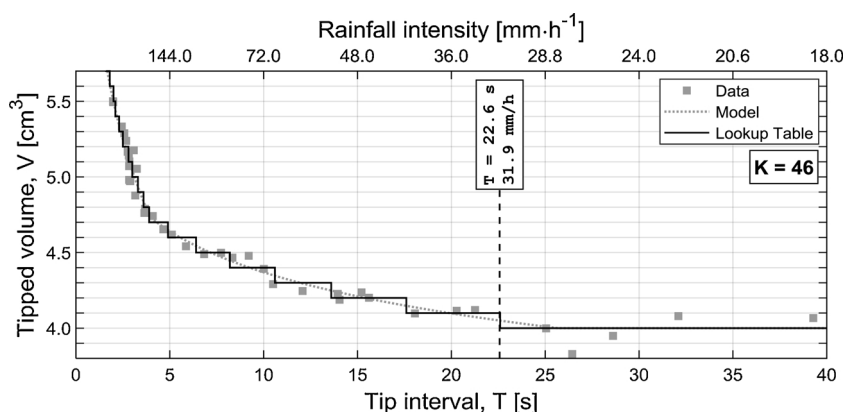


Fig. A1. The relationship between tipped water volume and tip interval alongside the calibration lookup table (under the assumption that recorded data are rounded to $\Delta V = 0.1 \text{ cm}^3$ and $\Delta T = 0.1 \text{ s}$). Rainfall intensities were calculated under the assumption that the collection area equalled 200 cm^2 .

Table A1

An example lookup table including volumetric corrections, $dV = V - V_0$, i.e. differences between actual tip volume and nominal volume, V_0 , generated based on the presented model Eq. (2), under the assumption that recorded data are rounded to $\Delta V = 0.1 \text{ cm}^3$ and $\Delta T = 0.1 \text{ s}$.

T	dV	T	dV	T	dV	T	dV	T	dV	T	dV	T	dV	T	dV	T	dV
0.1	4.9	2.6	1.2	5.1	0.6	7.6	0.5	10.1	0.4	12.6	0.3	15.1	0.2	17.6	0.1	20.1	0.1
0.2	4.1	2.7	1.2	5.2	0.6	7.7	0.5	10.2	0.4	12.7	0.3	15.2	0.2	17.7	0.1	20.2	0.1
0.3	3.6	2.8	1.1	5.3	0.6	7.8	0.5	10.3	0.4	12.8	0.3	15.3	0.2	17.8	0.1	20.3	0.1
0.4	3.3	2.9	1.1	5.4	0.6	7.9	0.5	10.4	0.4	12.9	0.3	15.4	0.2	17.9	0.1	20.4	0.1
0.5	3.1	3.0	1.0	5.5	0.6	8.0	0.5	10.5	0.4	13.0	0.3	15.5	0.2	18.0	0.1	20.5	0.1
0.6	2.8	3.1	1.0	5.6	0.6	8.1	0.5	10.6	0.3	13.1	0.3	15.6	0.2	18.1	0.1	20.6	0.1
0.7	2.7	3.2	1.0	5.7	0.6	8.2	0.4	10.7	0.3	13.2	0.3	15.7	0.2	18.2	0.1	20.7	0.1
0.8	2.5	3.3	0.9	5.8	0.6	8.3	0.4	10.8	0.3	13.3	0.3	15.8	0.2	18.3	0.1	20.8	0.1
0.9	2.4	3.4	0.9	5.9	0.6	8.4	0.4	10.9	0.3	13.4	0.3	15.9	0.2	18.4	0.1	20.9	0.1
1.0	2.3	3.5	0.9	6.0	0.6	8.5	0.4	11.0	0.3	13.5	0.3	16.0	0.2	18.5	0.1	21.0	0.1
1.1	2.2	3.6	0.8	6.1	0.6	8.6	0.4	11.1	0.3	13.6	0.2	16.1	0.2	18.6	0.1	21.1	0.1
1.2	2.1	3.7	0.8	6.2	0.6	8.7	0.4	11.2	0.3	13.7	0.2	16.2	0.2	18.7	0.1	21.2	0.1
1.3	2.0	3.8	0.8	6.3	0.6	8.8	0.4	11.3	0.3	13.8	0.2	16.3	0.2	18.8	0.1	21.3	0.1
1.4	1.9	3.9	0.7	6.4	0.5	8.9	0.4	11.4	0.3	13.9	0.2	16.4	0.2	18.9	0.1	21.4	0.1
1.5	1.8	4.0	0.7	6.5	0.5	9.0	0.4	11.5	0.3	14.0	0.2	16.5	0.2	19.0	0.1	21.5	0.1
1.6	1.7	4.1	0.7	6.6	0.5	9.1	0.4	11.6	0.3	14.1	0.2	16.6	0.2	19.1	0.1	21.6	0.1
1.7	1.7	4.2	0.7	6.7	0.5	9.2	0.4	11.7	0.3	14.2	0.2	16.7	0.2	19.2	0.1	21.7	0.1
1.8	1.6	4.3	0.7	6.8	0.5	9.3	0.4	11.8	0.3	14.3	0.2	16.8	0.2	19.3	0.1	21.8	0.1
1.9	1.6	4.4	0.7	6.9	0.5	9.4	0.4	11.9	0.3	14.4	0.2	16.9	0.2	19.4	0.1	21.9	0.1
2.0	1.5	4.5	0.7	7.0	0.5	9.5	0.4	12.0	0.3	14.5	0.2	17.0	0.2	19.5	0.1	22.0	0.1
2.1	1.4	4.6	0.7	7.1	0.5	9.6	0.4	12.1	0.3	14.6	0.2	17.1	0.2	19.6	0.1	22.1	0.1
2.2	1.4	4.7	0.7	7.2	0.5	9.7	0.4	12.2	0.3	14.7	0.2	17.2	0.2	19.7	0.1	22.2	0.1
2.3	1.3	4.8	0.7	7.3	0.5	9.8	0.4	12.3	0.3	14.8	0.2	17.3	0.2	19.8	0.1	22.3	0.1
2.4	1.3	4.9	0.6	7.4	0.5	9.9	0.4	12.4	0.3	14.9	0.2	17.4	0.2	19.9	0.1	22.4	0.1
2.5	1.2	5.0	0.6	7.5	0.5	10.0	0.4	12.5	0.3	15.0	0.2	17.5	0.2	20.0	0.1	22.5	0.1

Appendix B. Supplementary data

Supplementary material related to this article can be found, in the online version, at doi:<https://doi.org/10.1016/j.agrformet.2019.02.044>.

References

Bergmann, H., Breinhllter, H., Hahle, O., Krainer, R., 2001. Calibration of tipping bucket hyetographs. *Phys. Chem. Earth (C)* 26 (10–12), 731–736.

Borup, M., Grum, M., Linde, J.J., Mikkelsen, P.S., 2016. Dynamic gauge adjustment of high-resolution X-band radar data for convective rain storms: model-based evaluation against measured combined sewer overflow. *J. Hydrol.* 539, 687–699. <https://doi.org/10.1016/j.jhydrol.2016.05.002>.

Colli, M., Lanza, L.G., La Barbera, P., 2013. Performance of a weighing rain gauge under laboratory simulated time-varying reference rainfall rates. *Atmos. Res.* 131, 3–12. <https://doi.org/10.1016/j.atmosres.2013.04.006>.

Colli, M., Lanza, L.G., La Barbera, P., Chan, P.W., 2014. Measurement accuracy of weighing and tipping-bucket rainfall intensity gauges under dynamic laboratory testing. *Atmos. Res.* 144, 186–194. <https://doi.org/10.1016/j.atmosres.2013.08.007>.

DAVIS 6463, 2019. Stand Alone Rain Collectors. https://www.davisnet.com/product_documents/weather/spec_sheets/6463_6465_SS.pdf.

DAVIS 7852M, 2019. Stand Alone Rain Collectors. http://www.davisnet.com/product_documents/weather/spec_sheets/7857-7852_SS.pdf.

Duchon, C.E., Biddle, C.J., 2010. Undercatch of tipping-bucket gauges in high rain rate events. *Adv. Geosci.* 25, 11–15. <https://doi.org/10.5194/adgeo-25-11-2010>.

Eagleson, P.S., 1970. *Dynamic Hydrology*. McGraw-Hill, New York.

Fankhauser, R., 1998. Influence of systematic errors from tipping bucket rain gauges on recorded rainfall data. *Water Sci. Technol.* 37 (11), 121–129. [https://doi.org/10.1016/S0273-1223\(98\)00324-2](https://doi.org/10.1016/S0273-1223(98)00324-2).

Geiger, R., Aron, R.H., Todhunter, P., 1995. *The climate near the Ground*. Friedr. Vieweg & Sohn Verlagsgesellschaft mbH. Braunschweig/Wiesbaden.

Groisman, P.Y., Legates, D.R., 1994. The accuracy of United States precipitation data. *Bull. Am. Meteorol. Soc.* 75 (3), 215–224. [https://doi.org/10.1175/1520-0477\(1994\)075%3C0215:TAOUPS%3E2.0.CO;2](https://doi.org/10.1175/1520-0477(1994)075%3C0215:TAOUPS%3E2.0.CO;2).

Habib, E., Krajewski, W.F., Kruger, A., 2001. Sampling errors of tipping-bucket rain gauge measurements. *J. Hydrol. Eng.* 6, 159–166. [https://doi.org/10.1061/\(ASCE\)1084-0699\(2001\)6:2\(159\)](https://doi.org/10.1061/(ASCE)1084-0699(2001)6:2(159)).

Habib, E., Meselhe, E.A., Aduvala, A.V., 2008. Effect of local errors of tipping-bucket rain gauges on rainfall-runoff simulations. *J. Hydrol. Eng.* 13, 488–496. [https://doi.org/10.1061/\(ASCE\)1084-0699\(2008\)13:6\(488\)](https://doi.org/10.1061/(ASCE)1084-0699(2008)13:6(488)).

Hoffmann, M., Schwartengraber, R., Wessolek, G., Peters, A., 2016. Comparison of simple rain gauge measurements with precision lysimeter data. *Atmos. Res.* 174–175, 120–123. <https://doi.org/10.1016/j.atmosres.2016.01.016>.

Humphrey, M.D., Istok, J.D., Lee, J.Y., Hevesi, J.A., Flint, A.L., 1997. A new method for automated dynamic calibration of tipping-bucket rain gauges. *J. Atmos. Oceanic Technol.* 14, 1513–1519. [https://doi.org/10.1175/1520-0426\(1997\)014<1513:ANMFAD>2.0.CO;2](https://doi.org/10.1175/1520-0426(1997)014<1513:ANMFAD>2.0.CO;2).

La Barbera, P., Lanza, L.G., Stagi, L., 2002. Tipping bucket mechanical errors and their influence on rainfall statistics and extremes. *Water Sci. Technol.* 45, 1–9. <https://doi.org/10.2166/wst.2002.0020>.

Legates, D.R., Willmott, C.J., 1990. Mean seasonal and spatial variability in gauge corrected, global precipitation. *Int. J. Climatol.* 10, 111–127. <https://doi.org/10.1002/joc.3370100202>.

Michelson, D.B., 2004. Systematic correction of precipitation gauge observations using analyzed meteorological variables. *J. Hydrol.* 290, 161–177. <https://doi.org/10.1016/j.jhydrol.2003.10.005>.

Molini, A., Lanza, L.G., La Barbera, P., 2005. Improving the accuracy of tipping-bucket rain records using disaggregation techniques. *Atmos. Res.* 77, 203–217. <https://doi.org/10.1016/j.atmosres.2004.12.013>.

Nešpor, V., Sevruk, B., 1999. Estimation of wind-induced error of rainfall gauge measurements using a numerical simulation. *J. Atmos. Ocean. Technol.* 16, 450–464.

Ren, Z., Li, M., 2007. Errors and correction of precipitation measurements in China. *Adv. Atmos. Sci.* 24 (3), 449–458.

Seibert, J., Morén, A.-S., 1999. Reducing systematic errors in rainfall measurements using a new type of gauge. *Agric. For. Meteorol.* 98–99, 341–348.

Seo, D.-J., Siddique, R., Zhang, Y., Kim, D., 2014. Improving real-time estimation of heavy-to-extreme precipitation using rain gauge data via conditional bias-penalized optimal estimation. *J. Hydrol.* 519, 1824–1835. <https://doi.org/10.1016/j.jhydrol.2014.09.055>.

Sevruk, B., 1996. Adjustment of tipping-bucket precipitation gauge measurements. *Atmos. Res.* 42, 237–246.

Sevruk, B., Chvíla, B., 2005. Error sources of precipitation measurements using electronic weight systems. *Atmos. Res.* 77, 39–47.

Sevruk, B., Ondrás, M., Chvíla, B., 2009. The WMO precipitation measurement inter-comparisons. *Atmos. Res.* 92, 376–380.

Shedekar, V.S., King, K.W., Fausey, N.R., Soboyejo, A.B.O., Harmel, R.D., Brown, L.C.,

2016. Assessment of measurement errors and dynamic calibration methods for three different tipping bucket rain gauges. *Atmos. Res.* 178–179, 445–458. <https://doi.org/10.1016/j.atmosres.2016.04.016>.
- Shimizu, T., Kobayashi, M., Iida, S., Levia, D.F., 2018. A generalized correction equation for large tipping-bucket flow meters for use in hydrological applications. *J. Hydrol.* 563, 1051–1056. <https://doi.org/10.1016/j.jhydrol.2018.06.036>.
- Stahý, J., Czarnecka, H., Białuk, J. (Eds.), 1986. *Atlas Hydrologiczny Polski*. Wydawnictwo Geologiczne, Warszawa 1987.
- Stisen, S., Højberg, A.L., Trolborg, L., Refsgaard, J.C., Christensen, S.B., Olsen, M., Henriksen, H.J., 2012. On the importance of appropriate precipitation gauge catch correction for hydrological modelling at mid to high latitudes. *Hydrol. Earth Syst. Sci.* 16, 4157–4176.
- Vasvári, V., 2005. Calibration of tipping bucket rain gauges in the Graz urban research area. *Atmos. Res.* 77, 18–28. <https://doi.org/10.1016/j.atmosres.2004.12.012>.
- WMO, 2008. *Guide to Meteorological Instruments and Methods of Observation*. WMO-No. 8. World Meteorological Organization, Chairperson Publications Board.
- YOUNG 52202, 2019. *Tipping Bucket Rain Gauge Manual*. [http://www.youngusa.com/Manuals/52202-90\(J\)](http://www.youngusa.com/Manuals/52202-90(J)).